

doi:10.11835/j.issn.1674-4764.2015.03.011



# 直墙拱形巷道围岩应力场分析

唐 治, 潘一山, 朱小景, 崔乃鑫

(辽宁工程技术大学 矿山安全技术装备研究院; 力学与工程学院, 辽宁 阜新 123000)

**摘要:**为得出直墙拱形巷道围岩应力分布规律,应用复变函数弹性理论推导了直墙拱形巷道围岩应力分布的解析表达式。对直墙拱形巷道边界的围岩应力和巷道水平线方向的围岩应力分布规律进行分析,并考虑直墙拱形巷道断面高宽比和侧压系数对其影响规律。研究表明:在不同巷道断面高宽比、侧压系数下,直墙拱形巷道围岩应力集中区域主要集中在直墙底部底角处、拱形顶板中点附近和底板中部3个位置。不同巷道断面高宽比下,直墙拱形巷道沿水平线的应力分布规律基本相同。侧压系数大于1时,采用巷道断面高宽比小于1较有利于巷道稳定;侧压系数小于等于1时,采用巷道断面高宽比大于1较有利于巷道稳定。

**关键词:**直墙拱形巷道;复变函数;围岩应力

**中图分类号:**U451 **文献标志码:**A **文章编号:**1674-4764(2015)03-0079-07

## Analysis on surrounding rock stress field of vertical wall archy roadway

Tang Zhi, Pan Yishan, Zhu Xiaojing, Cui Naixin

(Technology &amp; Equipment of Coal Mine Safety, Liaoning Technical University,

School of Mechanics and Engineering, Liaoning Technical University, Fuxin 123000, Liaoning, P. R. China)

**Abstract:** The conformal transformation and elastic theory of complex function are used to derive the analytical expression of surrounding rock stress distribution of vertical wall archy roadway. The distribution laws of roadway boundary surrounding rock stress and the stress along horizontal line are analyzed. Also the impact of different aspect ratios of roadway cross-section and different lateral pressure coefficients on stress field of surrounding rocks are studied. The results show that: with different aspect ratios of roadway cross-section and different lateral pressure coefficients, three locations of vertical wall archy roadway surrounding rocks are main stress concentration area concentrated. The three locations are the basic angle at bottom of vertical wall, the location near midpoint of archy roof and the center of floor. Under different aspect ratios of roadway cross-section, the distribution laws of stress along horizontal line of vertical wall archy roadway are the same basically. When the lateral pressure coefficient is greater than one, roadway is stable with aspect ratio of roadway cross-section less than one. While, when the lateral pressure coefficient is not greater than 1, roadway is stable with aspect ratio of roadway cross-section greater than one.

**Key words:** vertical wall archy roadway; complex function; surrounding rock stress

**收稿日期:**2014-12-19

**基金项目:**国家自然科学基金(51374119, 51204090, 51174107)

**作者简介:**唐治(1983-),男,博士,主要从事矿山灾害力学研究,(E-mail)tangzhi0127@163.com。

**Received:**2014-12-19

**Foundation item:** National Natural Science Foundation of China(No. 51374119, 51204090, 51174107)

**Author brief:** Tang Zhi(1983-), PhD, main research interests: mine disaster mechanics, (E-mail)tangzhi0127@163.com.

煤矿巷道围岩应力大小和规律是巷道支护方式选取的重要依据之一。围岩应力大小不仅与煤矿采深、侧压系数等有关,还与巷道断面形状等相关(即使相同围岩条件下,围岩应力分布规律和围岩变形破坏规律也因巷道断面形状不同而不同)。直墙拱形断面巷道的断面由下部分矩形和上部分拱形组成,长期实践证明,直墙拱形断面巷道具有较好的稳定性,所以服务年限较长的巷道一般均采用直墙拱形断面巷道。了解和掌握巷道围岩应力分布规律对合理选择巷道支护方式具有重要的理论意义和实际应用价值。对于常规的圆形、椭圆形等巷道的围岩应力可以采用 Cauchy 积分法或幂级数法方便解出<sup>[1-3]</sup>,但复杂巷道围岩应力公式需借助复变函数弹性理论<sup>[4-6]</sup>及映射函数<sup>[7-9]</sup>。朱大勇等<sup>[10]</sup>求解了矩形断面围岩应力弹性解,赵凯等<sup>[11]</sup>利用多角形法得出了矩形洞室围岩应力,王润富<sup>[12]</sup>、刘金高等<sup>[13]</sup>求解了梯形孔口的应力,汤澄波等<sup>[14]</sup>、祝江鸿<sup>[15]</sup>分别利用复变函数法求解了天幕线拱形围岩应力和两个表示断面围岩应力的解析函数通式,但前提是能给出复杂断面映射函数。针对直墙拱形巷道围岩应力研究较少,对其他复杂巷道研究大多也只给出复杂巷道应力解析的隐函数,未给出巷道应力分布情况,也未对巷道断面高宽比和侧压系数对其影响规律进行深入分析。

## 1 模型建立

为简化计算,将巷道整个断面简化为以  $y$  轴为对称轴的六边形,无支护阻力,远场铅垂应力为  $\sigma_v$ ,水平应力为  $\sigma_h = k\sigma_v$ ,  $k$  为侧压系数,不计体力,计算模型如图 1 所示。设顶板宽为  $\overline{B_1A_1} = 2a$ ,底板宽为  $\overline{B_3A_3} = 2b$ ,断面总高度为  $\overline{DN} = 2h$ ,拱的高度为  $\overline{OD} = h_a$ ,直墙高为  $\overline{ON} = h_b = 2h - h_a$ ,直墙拱形断面高宽比  $c_0 = h/b$ 。以拱顶与直墙交界线和直墙拱形巷道断面的对称轴为  $x, y$  轴建立平面直角坐标系。以  $y$  轴为对称轴的六边形的顶点从右上方顺时针依次为  $A_1, A_2, A_3, B_3, B_2, B_1$ 。 $A_1, A_2, A_3$  处的外角分别为  $\vartheta_1 = \phi_1, \vartheta_2 = \phi_2, \vartheta_3 = \phi_3 = \frac{3\pi}{2}$ 。由几何关系可得出

$$\begin{aligned}\vartheta_1 &= \frac{3\pi}{2} - \arctan \frac{b-a}{2h-H}, \\ \vartheta_2 &= \pi + \arctan \frac{b-a}{2h-H}\end{aligned}\quad (1)$$

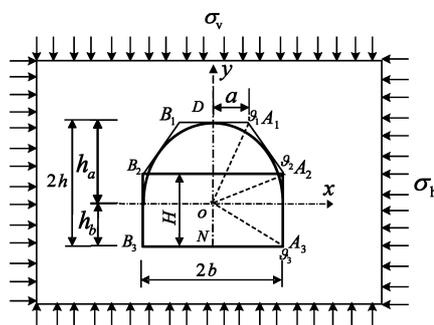


图 1 模型图

Fig. 1 diagram of model

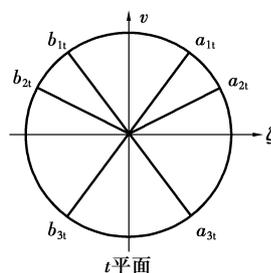


图 2 单位圆外域

Fig 2 The unit circle outland

## 2 直墙拱形巷道围岩应力解析

### 2.1 保角变换

首先将直墙拱形巷道围岩映射为单位圆形巷道围岩,即把图 1 中的六边形的外域部分映射为图 2 的单位圆外域部分。映射后  $A_1, A_2, A_3, B_3, B_2, B_1$  分别  $a_{1t}, a_{2t}, a_{3t}, b_{3t}, b_{2t}, b_{1t}$  与对应,如图 2。则有  $a_{1t} = ie^{-ik_1\pi}, a_{2t} = ie^{-ik_2\pi}, a_{3t} = ie^{-ik_3\pi}, b_{1t} = ie^{-ik_1\pi}, b_{2t} = ie^{-ik_2\pi}, b_{3t} = ie^{-ik_3\pi}$ 。其中  $K_1, K_2, K_3$  由六边形的尺寸确定。

由  $\vartheta_1 = \phi_1, \vartheta_2 = \phi_2, \vartheta_3 = \phi_3 = \frac{3\pi}{2}$  根据许瓦兹-克里斯托夫的多角映射理论,可得直墙拱形巷道映射函数为

$$z = \omega(t) = R \int_t \left( \frac{1 - i\lambda_1}{\tau} - \frac{1}{\tau^2} \right)^{\frac{\vartheta_1}{\pi} - 1} \left( \frac{1 - i\lambda_2}{\tau} - \frac{1}{\tau^2} \right)^{\frac{\vartheta_2}{\pi} - 1} \left( \frac{1 - i\lambda_3}{\tau} - \frac{1}{\tau^2} \right)^{\frac{\vartheta_3}{\pi} - 1} d\tau \quad (2)$$

式中:  $\lambda_1 = 2 \cos \kappa_1 \pi, \lambda_2 = 2 \cos \kappa_2 \pi, \lambda_3 = 2 \cos \kappa_3 \pi$ 。

作变量替换  $\tau = \frac{1}{T}$ , 可将  $t$  平面的单位圆外域映射为  $\zeta$  平面的单位圆内域, 得映射函数

$$z = \omega(\zeta) = -R \int_{\zeta} \frac{1}{T^2} (1 - i\lambda_1 T - T^2)^{\frac{\vartheta_1}{\pi} - 1} d\zeta$$

$$(1 - i\lambda_2 T - T^2)^{\frac{\vartheta_2}{\pi} - 1} (1 - i\lambda_3 T - T^2)^{\frac{\vartheta_3}{\pi} - 1} dT \quad (3)$$

设  $f(T) = f_1(T)f_2(T)f_3(T)$ ,  $f_1(T) = (1 - i\lambda_1 T - T^2)^{\varphi_1}$ ,  $\varphi_1 = \frac{\vartheta_1}{\pi}$ ,  $f_2(T) = (1 - i\lambda_2 T - T^2)^{\varphi_2}$ ,

$$\varphi_2 = \frac{\vartheta_2}{\pi} - 1, f_3(T) = (1 - i\lambda_3 T - T^2)^{\varphi_3}, \varphi_3 = \frac{\vartheta_3}{\pi} - 1.$$

将以下 3 个函数在零点的邻域内展开为级数, 得

$$f_1(T) = \sum_{k=0}^{\infty} \frac{f_1^{(k)}(0)}{k!} T^k = 1 + \sum_{k=0}^{\infty} C_{1k} T^k,$$

$$C_{1k} = \frac{f_1^{(k)}(0)}{k!}$$

$$f_2(T) = \sum_{k=0}^{\infty} \frac{f_2^{(k)}(0)}{k!} T^k = 1 + \sum_{k=0}^{\infty} C_{2k} T^k,$$

$$C_{2k} = \frac{f_2^{(k)}(0)}{k!}$$

$$f_3(T) = \sum_{k=0}^{\infty} \frac{f_3^{(k)}(0)}{k!} T^k = 1 + \sum_{k=0}^{\infty} C_{3k} T^k,$$

$$C_{3k} = \frac{f_3^{(k)}(0)}{k!}$$

所以,  $f(T) = f_1(T)f_2(T)f_3(T) = 1 + \sum_{k=0}^{\infty} B_k T^k$

其中  $B_k (k = 1, 2, \dots)$  由  $C_{1k}, C_{2k}, C_{3k}$  确定。

则式(3)为

$$z = \omega(\zeta) = -R \int_{\zeta} \frac{1}{T^2} (1 + \sum_{k=0}^{\infty} B_k T^k) dT = R \int_{\zeta} \left( -\frac{1}{T^2} - \sum_{k=0}^{\infty} B_k T^{k-2} \right) dT = R \left( \frac{1}{\zeta} - B_1 \ln \zeta - B_2 \zeta - \frac{B_3}{2} \zeta^2 - \frac{B_4}{3} \zeta^3 - \frac{B_5}{4} \zeta^4 - \dots \right) \quad (4)$$

为保证上式为单值函数, 应有  $B_1 = C_{11} + C_{21} + C_{31} = 0$ 。

由  $C_{11} = -i\lambda_1 \varphi_1, C_{21} = -i\lambda_2 \varphi_2, C_{31} = -i\lambda_3 \varphi_3$ ,  $\lambda_1 = 2 \cos \kappa_1 \pi, \lambda_2 = 2 \cos \kappa_2 \pi, \lambda_3 = 2 \cos \kappa_3 \pi$ , 得

$$\varphi_1 \cos \kappa_1 \pi + \varphi_2 \cos \kappa_2 \pi + \varphi_3 \cos \kappa_3 \pi = 0 \quad (5)$$

采用试算法, 先根据巷道几何尺寸确定  $\kappa_1 \pi, \kappa_2 \pi$ , 然后可由式(5)确定出  $\kappa_3 \pi$ 。

整理后得出直墙拱形巷道外域到单位圆内域的映射函数为

$$z = \omega(\zeta) = -R \left( \zeta - \frac{B_2}{\zeta} - \frac{B_3}{2\zeta^2} - \frac{B_4}{3\zeta^3} - \frac{B_5}{4\zeta^4} - \dots \right) \quad (6)$$

根据范广勤研究结果, 取前 5 项即可达到足够的精度, 且  $B_2, B_4$  为实数,  $B_3, B_5$  为纯虚数, 因此, 令

$B_2 = b_2, B_4 = b_4, B_3 = ib_3, B_5 = ib_5$ , 取前 5 项, 得

$$z = \omega(\zeta) = -R \left( \frac{1}{\zeta} - b_2 \zeta - \frac{ib_3}{2} \zeta^2 - \frac{ib_4}{3} \zeta^3 - \frac{ib_5}{4} \zeta^4 \right) \quad (7)$$

其中,  $b_i$  由  $c_{ij}$  表示,  $c_{l1} = -\lambda_l \varphi_l, c_{l2} = -\varphi_l \left[ 1 + \frac{\lambda_l^2}{2} (\varphi_l - 1) \right], c_{l3} = \lambda_l \varphi_l (\varphi_l - 1) \left[ 1 + \frac{\lambda_l^2}{6} (\varphi_l - 2) \right], c_{l4} = \lambda_l \varphi_l (\varphi_l - 1) \left[ \frac{1}{2} + \frac{\lambda_l^2}{2} (\varphi_l - 2) + \frac{\lambda_l^4}{24} (\varphi_l - 2)(\varphi_l - 3) \right], c_{l5} = \lambda_l \varphi_l (\varphi_l - 1) (\varphi_l - 2) \left[ \frac{1}{2} + \frac{\lambda_l^2}{6} (\varphi_l - 3) + \frac{\lambda_l^4}{120} (\varphi_l - 3)(\varphi_l - 4) \right], l = 1, 2, 3$ 。

在  $\zeta$  平面的单位圆周上,  $\rho = 1; \zeta = e^{i\varphi} = \cos \varphi + i \sin \varphi$ 。在  $z$  平面的六边形上,  $z_0 = x_0 + iy_0$ 。代入映射函数得

$$x_0 = R \left( \cos \varphi - b_2 \cos \varphi + \frac{b_3}{2} \sin 2\varphi - \frac{b_4}{3} \sin 3\varphi + \frac{b_5}{4} \sin 4\varphi \right)$$

$$y_0 = -R \left( \sin \varphi - b_2 \sin \varphi + \frac{b_3}{2} \cos 2\varphi - \frac{b_4}{3} \sin 3\varphi + \frac{b_5}{4} \cos 4\varphi \right) \quad (8)$$

$\zeta$  平面上点 ( $\rho = 1, \varphi = 0$ ), 与  $z$  平面巷道直墙上一点相对应, 其坐标为  $x_0 = b, y_0 = y_p$ , 得  $b = R \left( 1 - b_2 - \frac{b_4}{3} \right), y_p = -R \left( \frac{b_3}{2} + \frac{b_5}{4} \right), R = \frac{b}{1 - b_2 - \frac{b_4}{3}}$ 。当断面高宽比分别取 0.5、1、1.5 时,

保角变换参数如图 3。

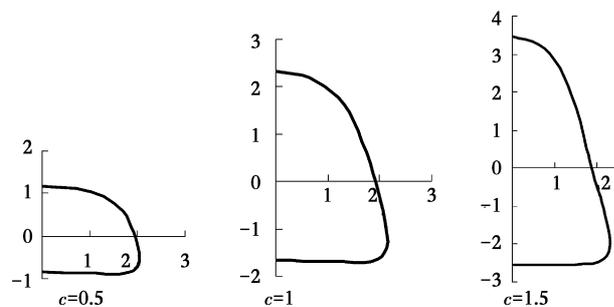


图 3 保角变换

Fig. 3 Conformal transformation

### 2.2 由边界条件确定

远场铅垂应力为  $\sigma_v$ 、水平应力为  $\sigma_h = k\sigma_v$ , 所以

$$\alpha = \frac{(1+k)\sigma_v}{4}, \alpha_1 = \frac{(1+k)\sigma_v}{2}, \beta_1 = 0.$$

因无支护阻力,  $X_s=Y_s=0, P_x=P_y=0$ , 则有

$$f_0 = -2\alpha\omega(\sigma) - (\alpha_1 - i\beta_1)\overline{\omega(\sigma)} \quad (9)$$

### 2.3 确定 $\varphi_0(\zeta)$ 、 $\psi_0(\zeta)$

由  $\varphi_0(\zeta) = \sum_{k=1}^{\infty} a_k \zeta^k$ , 可得  $\varphi_0'(\zeta) = \sum_{k=1}^{\infty} k a_k \zeta^{k-1}$ ,

$$\overline{\varphi_0'(\zeta)} = \sum_{k=1}^{\infty} k \overline{a_k} \frac{\rho^{2k-2}}{\zeta^{k-1}}, \frac{\omega(\zeta)}{\omega'(\zeta)} \overline{\varphi_0'(\zeta)}, \frac{\overline{\omega(\zeta)}}{\overline{\omega'(\zeta)}} \varphi_0'(\zeta),$$

$$\frac{1}{2\pi i} \int_{\sigma} \frac{\omega(\sigma)}{\omega'(\sigma)} \frac{\overline{\varphi_0'(\zeta)}}{\sigma - \zeta} d\sigma, \frac{1}{2\pi i} \int_{\sigma} \frac{\omega(\sigma)}{\omega'(\sigma)} \frac{\overline{\varphi_0'(\sigma)}}{\sigma - \zeta} d\sigma,$$

$$\frac{1}{2\pi i} \int_{\sigma} \frac{\overline{\omega(\sigma)}}{\overline{\omega'(\sigma)}} \frac{\varphi_0'(\sigma)}{\sigma - \zeta} d\sigma, \frac{1}{2\pi i} \int_{\sigma} \frac{f_0}{\sigma - \zeta} d\sigma, \frac{1}{2\pi i} \int_{\sigma} \frac{\overline{f_0}}{\sigma - \zeta} d\sigma$$

整理可得

$$\varphi_0(\zeta) = a_1 \zeta + ia_2 \zeta^2 + 2aR \left( \frac{b_4}{3} \zeta^3 + \frac{ib_5}{4} \zeta^4 \right) \quad (10)$$

$$\psi_0(\zeta) = -\frac{ib_5 a_1}{4\zeta^2} + \left( \frac{b_5 a_{2i}}{2} + \frac{b_4 a_1}{3} \right) \frac{1}{\zeta} +$$

$$R(\alpha_1 b_2 - 2\alpha)\zeta + \alpha_1 R \left( \frac{ib_3}{2} \zeta^2 + \frac{b_4}{3} \zeta^3 + \frac{ib_5}{4} \zeta^4 \right) +$$

$$\frac{\zeta^3 - b_2 \zeta + \frac{ib_3}{2} - \frac{b_4}{3\zeta} + \frac{ib_5}{4\zeta^2}}{1 + b_2 \zeta^2 + ib_3 \zeta^3 + b_4 \zeta^4 + ib_5 \zeta^5} \varphi_0'(\zeta) \quad (11)$$

### 2.4 确定 $\varphi(\zeta)$ 、 $\psi(\zeta)$

$$\varphi(\zeta) = \alpha\omega(\zeta) + \varphi_0(\zeta) =$$

$$\alpha R \left( \frac{1}{\zeta} - b_2 \zeta - \frac{ib_3}{2} \zeta^2 - \frac{b_4}{3} \zeta^3 - \frac{ib_5}{4} \zeta^4 \right) + \varphi_0(\zeta)$$

(12)

$$\psi(\zeta) = (\alpha_1 + i\beta_1)\omega(\zeta) + \psi_0(\zeta) =$$

$$\alpha_1 R \left( \frac{1}{\zeta} - b_2 \zeta - \frac{ib_3}{2} \zeta^2 - \frac{b_4}{3} \zeta^3 - \frac{ib_5}{4} \zeta^4 \right) + \psi_0(\zeta)$$

(13)

### 2.5 确定应力分量

$\Phi(\zeta) = \varphi'(\zeta)/\omega'(\zeta)$ ,  $\Psi(\zeta) = \psi'(\zeta)/\omega'(\zeta)$ , 可得直墙拱形巷道围岩应力分量的曲线坐标表达式

$$\sigma_{\varphi} + \sigma_{\rho} = 4Re[\Phi(\zeta)] = 4Re \left[ \alpha + \frac{\varphi_0'(\zeta)}{\omega'(\zeta)} \right] \quad (14)$$

$$\sigma_{\varphi} - \sigma_{\rho} + 2i\tau_{\varphi\rho} = \frac{2\zeta^2}{\rho^2 \omega'(\zeta)} [\overline{\omega(\zeta)}\Phi'(\zeta) + \omega'(\zeta)\Psi(\zeta)] =$$

$$\frac{2\zeta^2}{\rho^2 \omega'(\zeta)} \left\{ \frac{\omega(\zeta)}{\omega'(\zeta)} \left[ \frac{\varphi_0''(\zeta)}{\omega'(\zeta)} - \frac{\varphi_0'(\zeta)\omega''(\zeta)}{[\omega'(\zeta)]^2} \right] + \right. \\ \left. \omega'(\zeta) \left[ \alpha_1 + \frac{\psi_0'(\zeta)}{\omega'(\zeta)} \right] \right\} =$$

$$\frac{2\zeta^2}{\rho^2 \omega'(\zeta)} \left\{ \frac{\omega(\zeta)}{\omega'(\zeta)} \left[ \frac{\varphi_0''(\zeta)}{\omega'(\zeta)} - \frac{\varphi_0'(\zeta)\omega''(\zeta)}{[\omega'(\zeta)]^2} \right] + \right. \\ \left. \alpha_1 \omega'(\zeta) + \psi_0'(\zeta) \right\} \quad (15)$$

## 3 直墙拱形巷道围岩应力分析

### 3.1 直墙拱形巷道边界应力分布规律

巷道边界处,  $\rho = 1, \zeta = e^{i\varphi}, \sigma_{\rho} = \tau_{\varphi\rho} = 0$ 。取  $a = 1 \text{ m}, b = 2 \text{ m}$ , 当断面高宽  $c_0$  比分别取 0.5、1、1.5 时, 得直墙拱形巷道周边应力分布规律分别如图 4(a)、(b)、(c),  $-90^\circ \sim 90^\circ$  对应底板中点到顶板中点围岩边界。

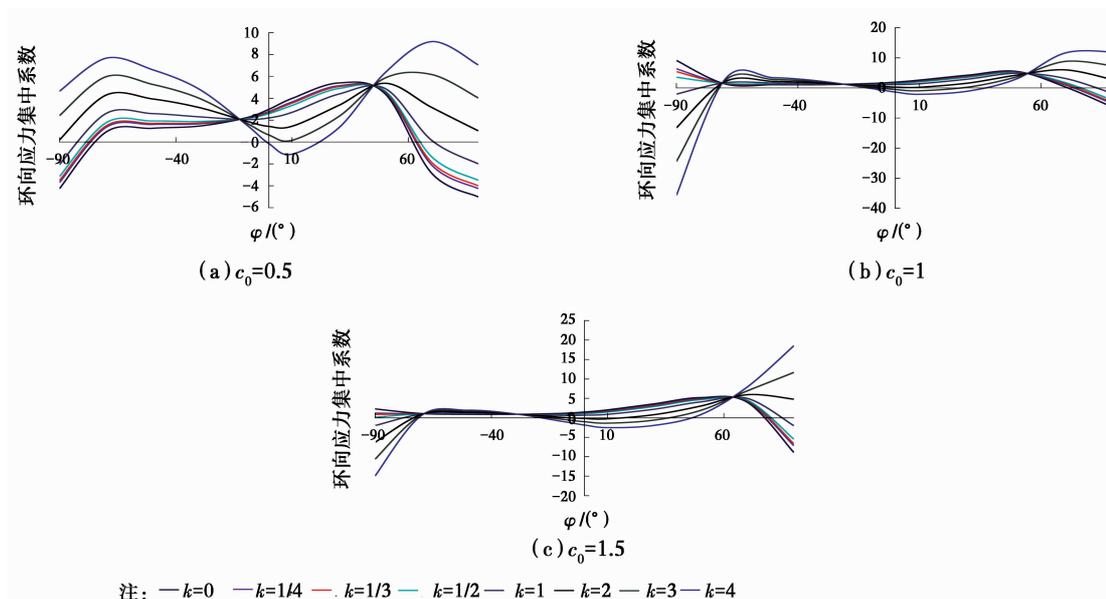


图 4 应力分布规律

Fig. 4 stress distribution law

从图 4(a) 可得: 巷道断面高宽比为 0.5 情况下, 侧压系数大于 1 时围岩边界环向应力有相同变化趋

势, 即底板中点到直墙底部再到直墙顶部的边界环向应力先增后减, 在直墙底部底角处区域出现较大应力

集中;直墙顶部到拱形顶板中点的边界环向应力先减后增再减。侧压系数小于 1 时,围岩边界环向应力也有相同变化趋势,即底板中点和顶板中点附近均出现拉应力,直墙底部到直墙顶部的边界环向应力较为恒定;直墙顶部到拱形顶板中点的边界环向应力先增后减然后变为拉应力。应力集中区域主要集中在直墙底部底角处和拱形顶板中点附近。

从图 4(b)可得:巷道断面高宽比为 1 情况下,侧压系数大于 1 时,围岩边界环向应力有相同变化趋势,即底板中点附近均出现拉应力,底板中点到直墙底部再到直墙顶部的边界环向应力先由拉应力变为压应力,然后增加后减小;直墙顶部到拱形顶板中点的边界环向应力先减后增再减。侧压系数小于 1 时,围岩边界环向应力也有相同变化趋势,即顶板中点附近均出现拉应力,底板中点到直墙底部再到

直墙顶部的边界环向应力先由逐渐减小;直墙顶部到拱形顶板中点的边界环向应力先增后减然后变为拉应力。应力集中区域主要集中在底板中部和拱形顶板中点附近,且拱形顶板应力集中系数小于底板。

从图 4(c)可得:巷道断面高宽比为 1.5 情况下,巷道围岩应力分布规律与巷道断面高宽比为 1 情况基本相同,不同之处在于拱形顶板应力集中系数大于底板,围岩应力分布比巷道断面高宽比为 1 时较好。

### 3.2 直墙拱形巷道沿水平线的应力分布规律

取  $\varphi = 0, \zeta = \rho$  为直墙拱形巷道水平线位置,由  $x = R(1 + c_1\rho^2 + c_3\rho^4)/\rho$  可将曲线坐标表示的应力分量表达式转换为直角坐标表示。取  $a = 1 \text{ m}, b = 2 \text{ m}$ ,断面高宽比  $c_0$  分别取 0.5、1、1.5 时,可得沿  $x$  轴围岩应力分布规律,如图 5(a)、(b)、(c)。

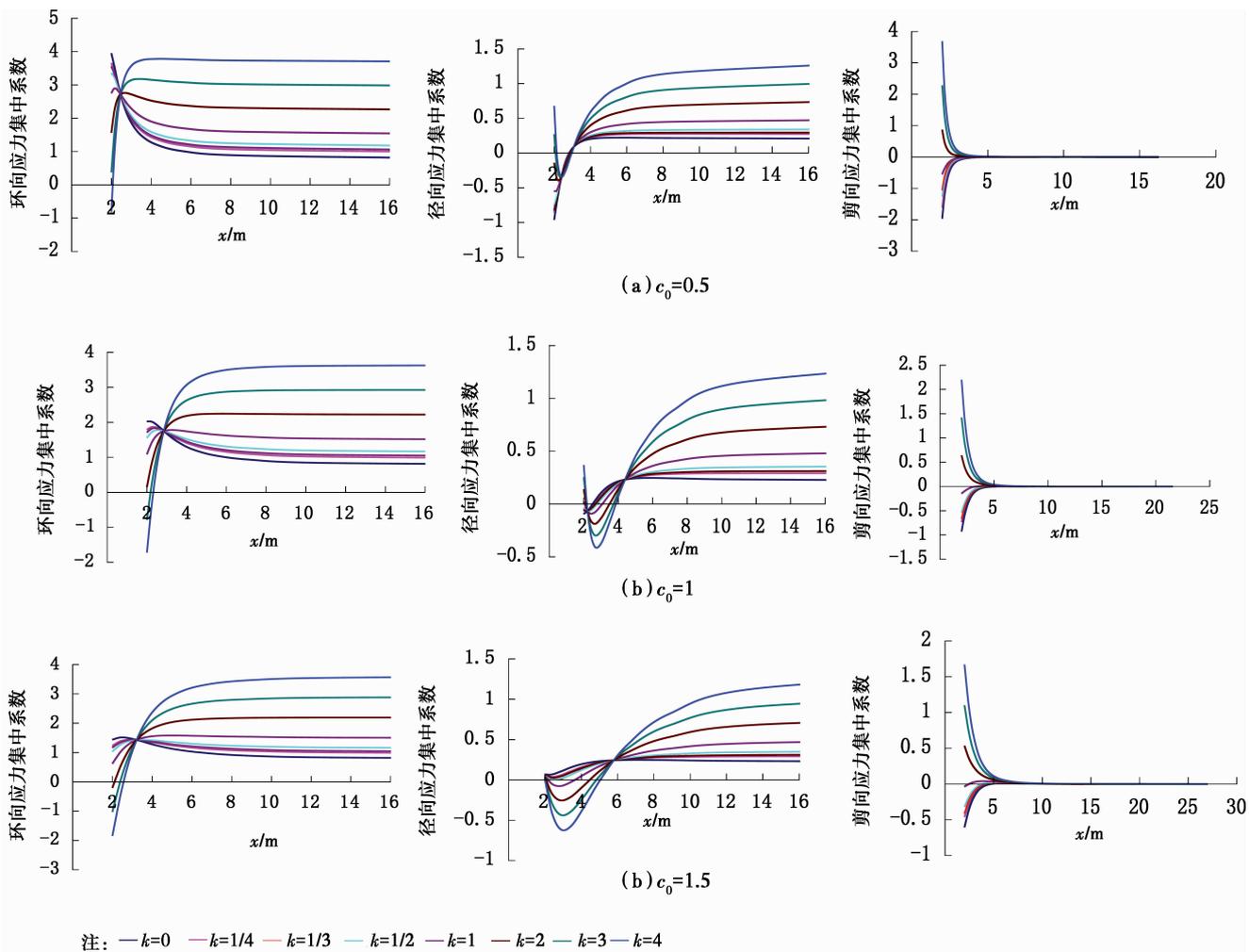


图 5 直角坐标下巷道周边应力分布规律

Fig. 5 Stress distribution rule of perimeter under rectangular coordinate

从图 5 可得:1)不同巷道断面高宽比下,直墙拱形巷道沿水平线的应力分布规律基本相同。2)侧压系数大于 1 时,不同巷道断面高宽比的环向应力均随至巷道边界距离增大而迅速增大,在距离巷道边界 2~4 m 后达到稳定;侧压系数小于 1 时,不同巷道断面高宽比的环向应力均随至巷道边界距离增大而先增大后减小,在距离巷道边界 1 m 左右达到最大值,然后较小并在距离巷道边界 2~4 m 后达到稳定。3)侧压系数大于 1 时,不同巷道断面高宽比的径向应力均随至巷道边界距离增大而先减小后变为拉应力然后增加,在距离巷道边界 4~6 m 后达到稳定;侧压系数小于 1 时,不同巷道断面高宽比的径向应力均随至巷道边界距离增大而增大,在距离巷道边界 2~4 m 后达到稳定。4)直墙拱形巷道边界 3 m 范围内出现了剪应力,剪应力随至巷道边界距离增大而迅速减小。当侧压系数大于 1 时,最大剪应力随侧压系数增加而增大;当侧压系数小于 1 时,最大剪应力随侧压系数增加而减小。

## 4 结论

1)采用保角变换,应用复变函数弹性理论推导了直墙拱形巷道围岩应力分布的解析表达式。

2)不同巷道断面高宽比、侧压系数下,直墙拱形巷道围岩应力集中区域均主要集中在直墙底部底角处、拱形顶板中点附近和底板中部 3 个位置。巷道断面高宽比一定情况下,侧压系数大于 1 时,围岩边界环向应力有相同变化趋势;采用巷道断面高宽比小于 1 较有利于巷道稳定;侧压系数小于等于 1 时,围岩边界环向应力也有相同变化趋势;采用巷道断面高宽比大于 1 较有利于巷道稳定。

3)道断面高宽比对直墙拱形巷道沿水平线的应力分布规律影响较小。侧压系数大于 1 时,巷道环向应力均随至巷道边界距离增大而迅速增大,径向应力均随至巷道边界距离增大而先减小后变为拉应力然后增加,最大剪应力随侧压系数增加而增大;侧压系数小于 1 时,巷道环向应力均随至巷道边界距离增大而先增大后减小,径向应力均随至巷道边界距离增大而增大,最大剪应力随侧压系数增加而减小。

## 参考文献:

[1] 王明斌,李术才,李树忱,等.圆形隧道围岩附加应力场的解析解答[J].岩土力学,2006,27(Sup):207-210.

- Wang M B, Li S C, Li S C, et al. Analytical solution of subsidiary stress field for circular tunnel [J]. *Rock and Soil Mechanics*, 2006, 27(Sup): 207-210. (in Chinese).
- [2] 卢文超,仲政,王旭.浅埋隧道围岩应力场的解析解[J].力学季刊,2003,24(1):50-54.
- Lu W C, Zhong Z, Wang X. Analytical solution for stress field in surrounding rocks of shallow tunnel [J]. *Journal of Chinese Quarterly Mechanics*, 2003, 24(1): 50-54. (in Chinese)
- [3] 蔡晓鸿,蔡勇斌,蔡勇平,等.二向不等围压和内压作用下椭圆形洞室的计算[J].地下空间与工程学报,2008,4(3):453-459.
- Cai X H, Cai Y B, Cai Y P, et al. Computation of elliptic tunnel under the combined action of two-dimensional unequal adjoining rock pressure and internal pressure [J]. *Chinese Journal Underground Space and Engineering*, 2008, 4(3): 453-459. (in Chinese)
- [4] Muskhelishvili N I. Some basic problems of the mathematical theory of elasticity: Fundamental equations, plane theory of elasticity, torsion and bending [M]. Groningen: P Noordhoff, 1953.
- [5] 陈子荫.围岩力学分析中的解析方法[M].北京:煤炭工业出版社,1994.
- Chen Z Y. Analytic method of mechanical analysis for the surrounding rock [M]. Beijing: Coal Industry Publishing House, 1994. (in Chinese)
- [6] Zhang Z Z, Sun Y Z. Analytical solution for a deep tunnel with arbitrary cross section in a transversely isotropic rock mass [J]. *International Journal of Rock Mechanics and Mining Sciences*, 2011, 48(8): 1359-1363.
- [7] 房营光,孙钧.地面荷载下浅埋隧道围岩的黏弹性应力和变形分析[J].岩石力学与工程学报,1998,17(3):239-247.
- Fang Y G, Sun J. Viscoelastic stress and deformation analysis of shallow tunnels under the load on the ground surrounding [J]. *Chinese Journal of Rock Mechanics and Engineering*, 1998, 17(3): 239-247. (in Chinese)
- [8] 朱大勇,钱七虎,周早生,等.复杂形状洞室映射函数的新解法[J].岩石力学与工程学报,1999,18(3):279-282.
- Zhu D Y, Qian Q H, Zhou Z S, et al. New method for calculating mapping function of opening with complex shape [J]. *Chinese Journal of Rock Mechanics and Engineering*, 1999, 18(3): 279-282. (in Chinese)
- [9] 皇甫鹏鹏,伍法权,郭松峰,等.基于边界点搜索的洞室外域映射函数求解法[J].岩石力学,2011,32(5):1418-

- 1424.
- Huangfu P P, Wu F Q, Guo S F, et al. A new method for calculating mapping function of external area of cavern with arbitrary shape based on searching points on boundary [J]. *Rock and Soil Mechanics*, 2011, 32 (5): 1418-1424. (in Chinese)
- [10] 朱大勇, 钱七虎, 周早生, 等. 复杂形状洞室围岩应力弹性解析分析[J]. *岩石力学与工程学报*, 1999, 18(4): 402-404.
- Zhu D Y, Qian Q H, Zhou Z S, et al. Elastic solution to stresses of rock masses around openings with complex shape [J]. *Chinese Journal of Rock Mechanics and Engineering*, 1999, 18(4): 402-404. (in Chinese)
- [11] 赵凯, 刘长武, 张国良. 用弹性力学的复变函数法求解矩形洞室周边应力[J]. *采矿与安全工程学报*, 2007, 24(3): 361-365.
- Zhao K, Liu C W, Zhang G L. Solution for perimeter stresses of rocks around a rectangular chamber using the complex function of elastic mechanics [J]. *Journal of Mining & Safety Engineering*, 2007, 24(3): 361-365. (in Chinese)
- [12] 王润富. 弹性力学的复变函数计算机解[J]. *河海大学学报*, 1991, 19(2): 71-74.
- Wang R F. Computer solutions for complex function in elasticity [J]. *Journal of Hohai University*, 1991, 19(2): 71-74. (in Chinese)
- [13] 刘金高, 王润富. 马蹄形孔口和梯形孔口的应力集中问题[J]. *岩土工程学报*, 1995, 17(5): 57-63.
- Liu J G, Wang R F. The stress concentration of U-shaped and ladder-shaped holes [J]. *Chinese Journal of Geotechnical Engineering*, 1995, 17(5): 57-63. (in Chinese)
- [14] 汤澄波, 范广勤. 高地应力区天幕线拱形洞室断面的解法[J]. *煤炭工程*, 1989(1): 16-18.
- Tang C B, Fan G Q. Determination of the mapping function for the exterior do-main of a non-circular opening by means of the multiplication of tree absolutely convergent series [J]. *Coal Engineering*, 1989(1): 16-18. (in Chinese)
- [15] 祝江鸿. 隧洞围岩应力复变函数分析法中的解析函数求解[J]. *应用数学和力学*, 2013, 34(4): 346-354.
- Zhu J H. Rock for caverns with the complex variable theory [J]. *Applied Mathematics and Mechanics*, 2013, 34(4): 346-354. (in Chinese)

(编辑 王秀玲)